JACS
JOURNAL OF THE AMERICAN CHEMICAL SOCIETY
Article
pubs.acs.org/JACS

Studies into the Mechanism of CO-Induced N_2 Cleavage Promoted by an *Ansa*-Hafnocene Complex and C−C Bond Formation from an Observed Intermediate

Donald J. Knobloch,[†] Scott P. Semproni,[‡] Emil Lobkovsky,[†] and Paul J. Chirik*[,†,‡]

[†]Department of Chemistry and Chemical Biology, Cornell University, Ithaca, New York 14853, United States
[‡]Department of Chemistry, Princeton University, Princeton, New Jersey 08544, United States

Supporting Information

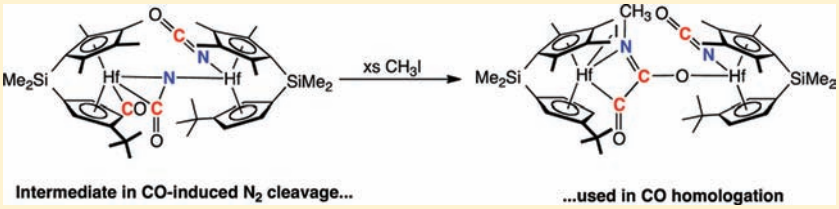

ABSTRACT: Carbonylation of the hafnocene dinitrogen complex, $[Me_2Si(\eta^5\text{-}C_5Me_4)(\eta^5\text{-}C_5H_3\text{-}^t\!Bu)Hf]_2(\mu_2, \eta^2, \eta^2\text{-}N_2)$, yields the corresponding hafnocene oxamidide compound, arising from N_2 cleavage with concomitant C−C and C−N bond formation. Monitoring the addition of 4 atm of CO by NMR spectroscopy allowed observation of an intermediate hafnocene complex with terminal and bridging isocyanates and a terminal carbonyl. ^{13}C labeling studies revealed that the carbonyl is the most substitutionally labile ligand in the intermediate and that N−C bond formation in the bridging isocyanate is reversible. No exchange was observed with the terminal isocyanate. Kinetic data established that the conversion of the intermediate to the hafnocene oxamidide was not appreciably inhibited by carbon monoxide and support a pathway involving rate-determining C−C coupling of the isocyanate ligands. Addition of methyl iodide to the intermediate hafnocene resulted in additional carbon−carbon bond formation arising from CO homologation following nitrogen methylation. Similar reactivity with ^{t}BuNCO was observed where C−C coupling occurred upon cycloaddition of the heterocumulene. By contrast, treatment of the intermediate hafnocene with CO_2 resulted in formation of a μ-oxo hafnocene with two terminal isocyanate ligands.

INTRODUCTION

The cleavage and functionalization of atmospheric nitrogen is a long-standing challenge in synthetic chemistry.[1] Terrestrial and bioavailable ammonia are prepared by fixing atmospheric nitrogen either with the industrial Haber−Bosch process[2] or naturally with the nitrogenase family of enzymes.[3] Dinitrogen functionalization with soluble transition metal complexes offers the opportunity to explore mechanistic pathways and tune ligand environments to open new reactivity for elaboration of the strong N≡N bond.[4] Methods for dinitrogen cleavage include nitride formation through bimetallic cooperativity where two metals provide the reducing equivalents[5,6] or by proton coupled electron transfer to yield ammonia.[7] Schrock[8] and, more recently, Nishibayashi[9] have evolved the latter strategy into a catalytic process for ammonia synthesis. Homogeneous complexes that promote N−H bond formation from H_2 addition[10a] and complete hydrogenation to ammonia are also known.[10b,c]

Ligand-induced dinitrogen cleavage, whereby an added ligand serves the dual purpose of supplying reducing equivalents and forming new bonds to nitrogen, is an attractive and potentially versatile strategy for N_2 functionalization. Fryzuk and co-workers have pioneered this strategy in tantalum chemistry and have reported several examples of N_2 functionalization and cleavage with both main group and transition metal hydrides.[11] Our laboratory has reported the extension of this concept to N−C bond forming reactions with zirconium and hafnium. Carbonylation of the *ansa*-hafnocene dinitrogen complex, $[Me_2Si(\eta^5\text{-}C_5Me_4)(\eta^5\text{-}C_5H_3\text{-}^t\!Bu)Hf]_2(\mu_2, \eta^2, \eta^2\text{-}N_2)$ (**1**), resulted in N_2 bond cleavage with concomitant formation of one C−C and two N−C bonds.[12] At higher CO pressures (~4 atm), a C_2 symmetric product, **2-C$_2$**, was obtained while, at lower pressures (~1 atm), the C_1 symmetric isomer, **2-C$_1$**, was observed (Scheme 1). Carbon monoxide induced dinitrogen cleavage[13] appears to be general among group 4 metallocenes with strongly activated dinitrogen ligands,[14] and synthesis of various free alkyl-substituted oxamides has been accomplished.[15] This strategy has also been applied to silylated dinitrogen cores and used in the synthesis of formamide from N_2, CO, $CySiH_3$, and a proton source.[16]

Understanding the mechanism of oxamidide formation is desirable to expand the scope of the reaction and ultimately develop insights for the evolution of a catalytic cycle. In our initial report,[12] addition of a stoichiometric amount of CO yielded the cyclometalated hafnocene, **3**, arising from CO-induced

Received: September 10, 2011
Published: February 10, 2012

   dx.doi.org/10.1021/ja208562d | J. Am. Chem.Soc. 2012, 134, 3377−3386

Scheme 1. CO-Induced N_2 Cleavage with an *Ansa*-Hafnocene Complex

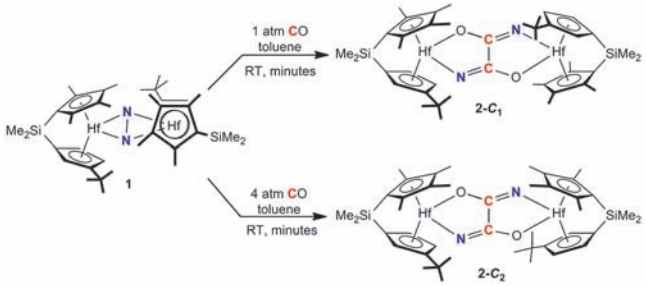

N_2 cleavage, N−C bond formation, and C−H activation (Scheme 2). Isolation of **3** implicated the formation of a dihafnocene intermediate with a briding nitrido that promoted

Scheme 2. Coupling CO-Induced N_2 Cleavage to N−H Bond Formation

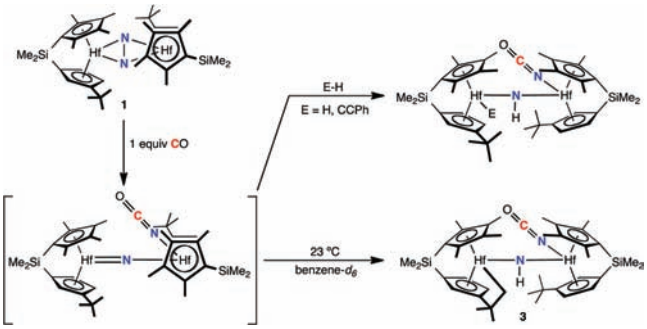

1,2-addition of the *tert*-butyl C−H bond and also suggested that N−N bond cleavage was not the step with the highest activation barrier en route to the hafnocene oxamidides, **2-C$_1$** and **2-C$_2$**. Support for the μ-nitrido dihafnocene intermediate was provided by the interception of this species by intermolecular 1,2-addition of dihydrogen and the C−H bonds of terminal alkynes (Scheme 2).[14]

Concurrent with these studies, Schwarz and co-workers reported DFT calculations aimed at exploring the mechanism of formation of **2-C$_1$**, **2-C$_2$**, and **3**.[17] The preferred pathway for hafnocene oxamidide formation commenced with CO coordination and insertion into a Hf−N bond. At relatively high carbon monoxide pressures, a second coordination−insertion event occurs which was computed to form a C_2 symmetric intermediate. This species undergoes homolytic N−N cleavage to form a hafnocene isocyanate complex that couples to form the oxamidide core. For **3**, a pathway involving a dihafnocene μ-nitrido complex was favored and its reactivity with H_2 was predicted prior to publication of the experimental studies.

While the pathway from **1** to **3** with stoichiometric carbon monoxide is now well understood, the formation of the hafnocene oxamidide products arising from 2 equiv of CO has not been experimentally examined. Formation of **3** and related complexes formed from 1,2-addition of E−H bonds established fast N−N bond cleavage through a transient bridging nitrido, but little is known about the C−C bond-forming step and the origin of the pressure dependence on isomer formation. Here we describe studies into the mechanism of CO-induced N_2 cleavage to yield hafnocene oxamidide complexes. We also report spectroscopic characterization of an intermediate, establish the reversibility of the N−C bond formations, and disclose new CO homologation reactions.

RESULTS AND DISCUSSION

In our initial report on CO-induced N_2 bond cleavage with **1**, definitive structural characterization of the C_1 symmetric hafnocene oxamidide complex, **2-C$_1$**, was elusive. Without definitive structural characterization, determination of the mechanistic rationale for the observed pressure dependence was challenging, if not impossible. Based on the available NMR data, we[12] and Schwarz[17] speculated on the stereochemistry of the observed isomer although a definitive assignment could not be made in the absence of crystallographic data. We have since obtained single crystals of **2-C$_1$**. A representation of the (*S*, *S*) enantiomer of the molecular structure is presented in Figure 1.

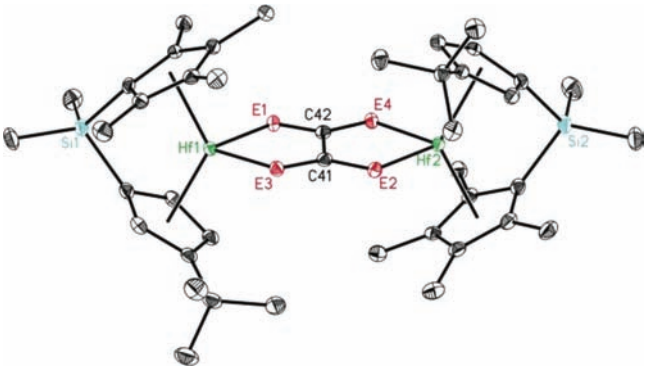

Figure 1. Solid state structure of (*S*, *S*)-**2-C$_1$** at 30% probability ellipsoids. Hydrogen atoms omitted for clarity.

Representations of the (*R*, *R*) enantiomer of this and all structures in this work are presented in the Supporting Information. As was observed with **2-C$_2$**, the wedges of each hafnocene are nearly coplanar with a dihedral angle of 12.5°. The nitrogen and oxygen atoms in the $[N_2C_2O_2]^{4-}$ core could not be distinguished and are designated "E" in the structure. A similar ambiguity occurred in the solid state structure of $[(\eta^5\text{-}C_5Me_4H)_2Hf]_2(N_2C_2O_2)$.[14] For **2-C$_1$**, the bond distances of the core in combination with NMR spectroscopic data establish a pseudo *trans* pairwise relationship where E(1) and E(2) have the same identity as do E(3) and E(4). Thus the oxamidide cores in both **2-C$_1$** and **2-C$_2$** are the same; the difference in the two isomers arises from the relative orientation of the *ansa*-cyclopentadienyl ligands. In **2-C$_2$**, the rings are oriented such that the *tert*-butyl groups are *syn* with respect to each other. By contrast, these substituents in **2-C$_1$** are geared in an *anti* arrangement placing one *tert*-butyl *syn* to an oxygen and the other *syn* to nitrogen. This eliminates any symmetry elements.

Because crystallographic characterization of **2-C$_1$** did not distinguish between the O and N atoms of the oxamidide core, additional proof was sought. Previously our laboratory has established that heterocumulenes such as CO_2 and ^{t}BuNCO undergo clean cycloaddition exclusively at the Hf−N bonds of oxamadide complexes.[15] Addition of 2 equiv of ^{t}BuNCO to a toluene solution of **2-C$_1$** cleanly yielded the desired product, **2-C$_1$-(^{t}BuNCO)$_2$**, arising from cycloaddition of the isocyanate. The solid-state structure was determined by X-ray diffraction (Figure 2) and established a *transoid* relationship between the nitrogen atoms in the core of the molecule. Other structural and spectroscopic properties are consistent with the previously

dx.doi.org/10.1021/ja208562d | J. Am. Chem.Soc. 2012, 134, 3377−3386

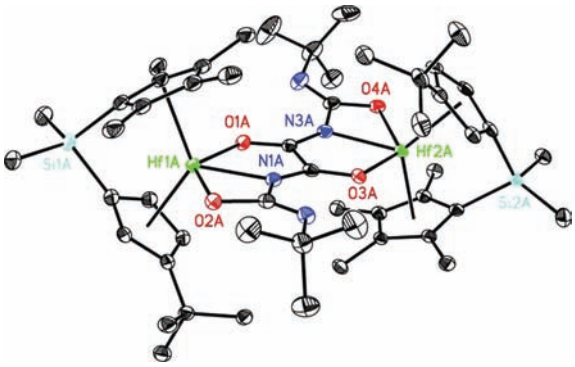

Figure 2. Solid state structure of (*S*, *S*)-**2-C$_1$**-(**^{t}BuNCO**)$_2$ at 30% probability ellipsoids. Hydrogen atoms omitted for clarity.

characterized C_2 symmetric isomer.[15] As it is also unlikely these additions would induce isomerization of the hafnocene oxamidide core, the nitrogen atoms in **2-C$_1$** are almost certainly *transoid*. This geometry has been consistently observed in all zirconocene and hafnocene oxamidide complexes prepared to date.

In an attempt to detect intermediates during oxamidide formation, the carbonylation of **1** was performed at 0 °C and monitored in situ by NMR spectroscopy. Addition of 4 atm of CO to a toluene-d_8 solution of **1** revealed formation of a new C_1 symmetric hafnocene compound, **Int**. Warming the sample to 23 °C in the presence of 4 atm of CO resulted in the clean and quantitative conversion of **Int** exclusively to **2-C$_2$**. Repeating the carbonylation of **1** with 4 atm CO to form **Int** followed by evacuation of the headspace produced a 3:1 mixture of **2-C$_2$** and **2-C$_1$**. Attempts to convert **Int** to exclusively **2-C$_1$** under a variety of conditions were unsuccessful; mixtures of the two isomeric hafnocene oxamidides were consistently and reproducibly observed. Under all pressure conditions examined, only one isomer of **Int** was detected by NMR spectroscopy.

Characterization of **Int** was accomplished by multinuclear (^{1}H, ^{13}C, ^{15}N) NMR and infrared spectroscopies. Combinations of ^{13}C and ^{15}N isotopologues were prepared in a straightforward manner using ^{13}CO and ^{15}N$_2$ gases, respectively. Unfortunately, the transient nature of **Int** has thus far precluded the growth of single crystals. However, isolation of the compound in the solid state was accomplished by lyophilization of a benzene solution on the high vacuum line.

The toluene-d_8 {^{1}H}^{13}C NMR spectrum of **Int-^{13}C$_3$-^{15}N$_2$** (the subscripts denote the number of isotopically labeled atoms in the molecule) is presented in Figure 3 and exhibited three resonances, indicating *three* inequivalent carbonyl ligands in the structure. Two of the carbons are bonded to nitrogen as evidenced by the observation of $^1J_{C-N}$ couplings in two of the peaks. The ^{13}C resonance centered at 134.48 ppm ($^1J_{C-N}$ = 32.9 Hz) is diagnostic of a terminal isocyanate bound to hafnium while the second resonance at 192.50 ppm ($^1J_{C-N}$ = 9.6 Hz) is assigned as a rare example of a bridging isocyanate. Nitrogen−carbon bond formation was also confirmed by ^{15}N NMR spectroscopy. Resonances were observed at 89.6 and 241.1 ppm for the terminal and bridging isocyanate ligands, respectively. The presence of a terminal isocyanate was also supported by the observation of a strong [NCO] stretch at 2220 cm^{-1} in the solid state (KBr) infrared spectrum.

The third unique carbon environment, centered at 247.07 ppm, is coupled to the bridging isocyanate ($^2J_{C-C}$ = 13.7 Hz)

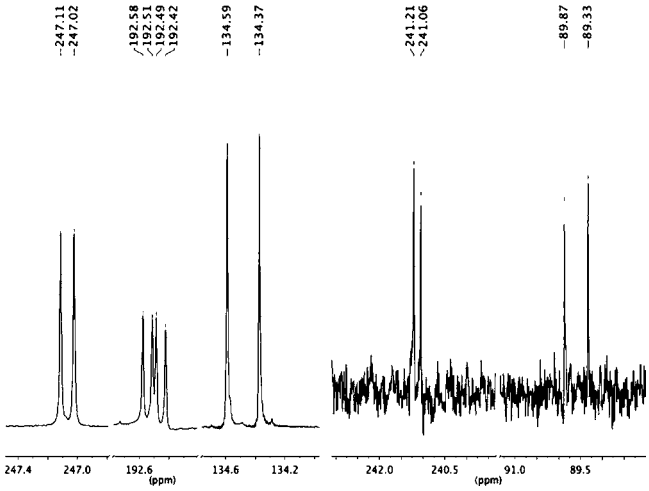

Figure 3. Partial {^{1}H}^{13}C (left) and ^{15}N (right) NMR spectra of **Int-^{13}C$_3$-^{15}N$_2$** in toluene-d_8 at 23 °C.

and exhibits no coupling to ^{15}N. These data, in combination with the observation of a strong IR band at 1959 cm^{-1} (KBr), support assignment as a terminal carbonyl ligand. The observation of C−C coupling through the hafnium center is unusual. Through metal C−H coupling has been observed in group 4 metallocene chemistry by Bercaw and co-workers in (η^5-C$_5$Me$_5$)$_2$ZrH$_2$(CO) ($^2J_{C-H}$ = 25 Hz)[18] and (η^5-C$_5$Me$_5$)$_2$HfH$_2$(CO) ($^2J_{C-H}$ = 25 Hz).[19] Our laboratory has observed through metal H−H coupling in the zirconocene hydride, [Me$_2$Si(η^5-C$_5$Me$_4$)(η^5-C$_5$H$_3$-3-^{t}Bu)ZrH$_2$]$_2$ ($^2J_{H-H}$ = 7 Hz).[20] Similarly, Wilkinson and co-workers observed H−H coupling ($^2J_{H-H}$ = 10 Hz) in the tantalocene trihydride, (η^5-C$_5$H$_5$)$_2$TaH$_3$.[21] To our knowledge, however, through metal C−C coupling has not been reported. No such coupling was observed in the ^{13}C NMR spectra of Me$_2$Si(η^5-C$_5$Me$_4$)(η^5-C$_5$H$_3$-3-^{t}Bu)Hf(^{13}CO)$_2$ and Me$_2$Si(η^5-C$_5$Me$_4$)(η^5-C$_5$H$_3$-3-^{t}Bu)-Hf(^{13}CH$_3$)$_2$.

Based on these data, the preferred structure of **Int**, shown in Figure 4, is a dihafnocene complex containing terminal

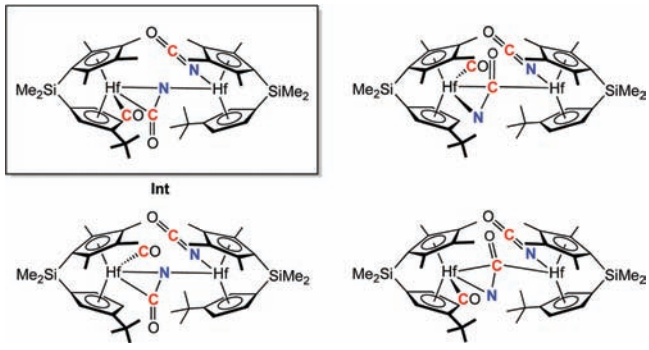

Figure 4. Preferred structure (boxed) of **Int** and possible alternatives.

isocyanate and carbonyl ligands along with a bridging isocyanate. Because of the C_1 symmetric nature of the *ansa*-bis(cyclopentadienyl) ligand environment coupled with the reactivity and instability of the compound, the stereochemical arrangement of the ligands in the metallocene wedge with respect to the cyclopentadienyl substituents has not been definitively established crystallographically. However, subsequent isotopic exchange and reactivity studies (*vide infra*)

dx.doi.org/10.1021/ja208562d | *J. Am. Chem.Soc.* 2012, 134, 3377−3386

Scheme 3. Isotopic Exchange Studies with Int-$^{13}C_3$ and Natural Abundance CO

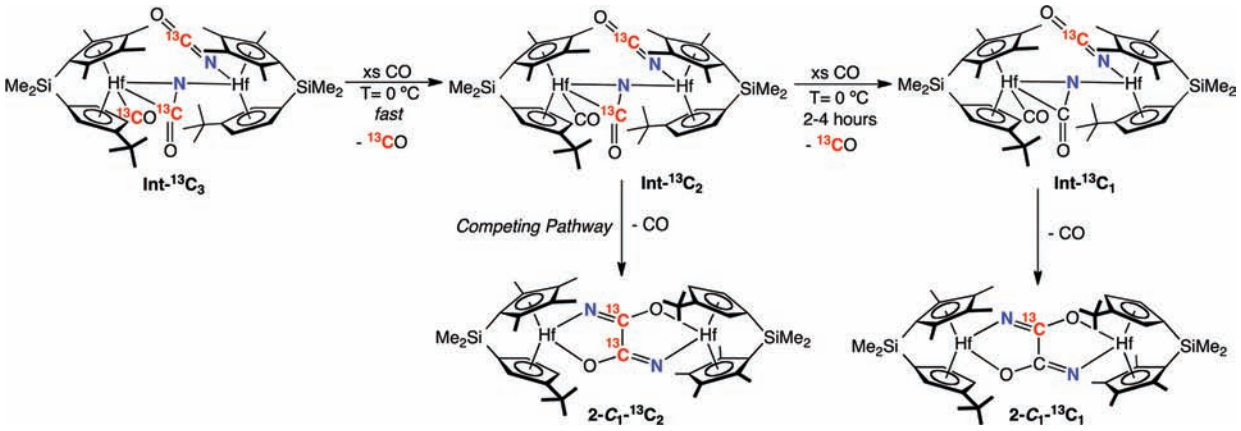

provide substantial experimental support for the preferred structure presented in Figure 4.

Isotopic exchange studies were conducted to gain an understanding into the C−C bond forming step, determine the reversibility of N−C bond formation, and establish the fate of the terminal CO and bridging [NCO] ligands. Exposure of a frozen toluene-d_8 solution of **Int**-$^{13}\mathbf{C}_3$ to approximately 4 atm of natural abundance CO gas resulted in complete exchange of the terminal carbonyl ligand over the course of 90 min at 0 °C (Scheme 3). In the $\{^1H\}^{13}C$ NMR spectrum (Figure 5) of the resulting **Int**-$^{13}\mathbf{C}_2$ isotopomer, the signal at 247.07 ppm for the terminal CO ligand has disappeared as has the $^2J_{C-C}$ coupling in the bridging isocyanate resonance. Once isotopic exchange was complete, the contents of the tube were again frozen and the excess CO/^{13}CO in the headspace removed. The solution was thawed, and **Int**-$^{13}\mathbf{C}_2$ was allowed to convert to a mixture of **2**-$\mathbf{C}_1$ and **2**-$\mathbf{C}_2$ oxamidide products. Analysis of the mixture by ^{13}C NMR spectroscopy established the formation of **2**-$\mathbf{C}_1$-$^{13}\mathbf{C}_2$. The isotopologue with only one isotopically labeled oxamidide carbon, **2**-$\mathbf{C}_1$-$^{13}\mathbf{C}_1$, was not detected. The symmetry of this isomer of the product allows disambiguation between incorporation of one and two equivalents of ^{13}C label. This is not possible for the C_2 symmetric compound, **2**-$\mathbf{C}_2$. In the previous experiment the ^{13}C label was detected in the C_2 symmetric isomer. These results establish that coupling of the bridging and terminal isocyanates is responsible for oxamidide formation.

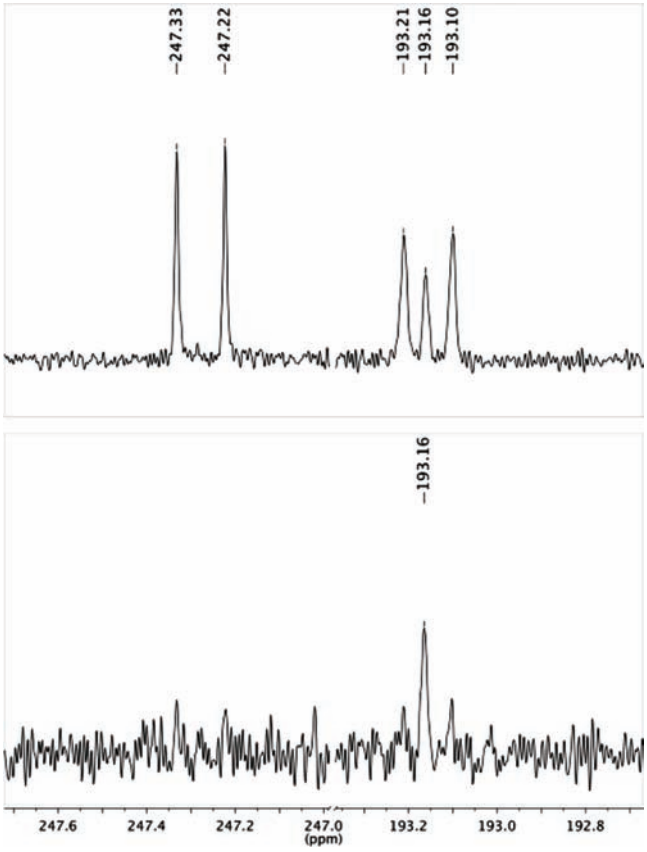

Figure 5. Toluene-d_8 $\{^1H\}^{13}C$ NMR spectrum of the addition of natural abundance CO to **Int**-$^{13}\mathbf{C}_3$ after 5 min (top) and 1 h (bottom).

The lability of the terminal carbonyl ligand in **Int** was also confirmed by infrared spectroscopy. The solid state (KBr) spectrum of **Int** following treatment with 1 atm of ^{13}CO exhibited a strong band centered at 1913 cm^{-1}, the appropriate isotopic shift expected from the harmonic oscillator model for the terminal carbonyl ligand. The band observed at 1959 cm^{-1} for the natural abundance material was absent in the spectrum of the material isolated after exposure to ^{13}CO gas.

A second ^{13}C labeling experiment was conducted to determine the reversibility of isocyanate formation. The labeling experiment described above, namely addition of natural abundance CO to **Int**-$^{13}\mathbf{C}_3$, was repeated over a longer time scale. Monitoring the progress of the reaction by ^{13}C NMR spectroscopy revealed the gradual disappearance of the resonance centered at 193.16 ppm for the bridging isocyanate ligand over the course of 4 h at 0 °C. Importantly, no isotopic exchange was observed in the terminal isocyanate ligand over this time period or longer reaction times (Scheme 3).

Warming the mixture of ^{13}C isotopologues of **Int** yielded a mixture of labeled hafnocene oxamidides (Scheme 3). As exchange of carbon monoxide with the bridging isocyanate is competitive with formation of the final product, **2**-$\mathbf{C}_1$-$^{13}\mathbf{C}_2$ was observed. In addition, the hafnocene isotopologue with only one isotopic label, **2**-$\mathbf{C}_1$-$^{13}\mathbf{C}_1$, was also observed by ^{13}C NMR spectroscopy (see Supporting Information). These results establish the reversibility of N−C bond formation in the bridging isocyanate but not in the terminal one. These data again support coupling of these two ligands is responsible for the formation of the oxamidide core.

The observation of **Int** as an intermediate on the pathway to hafnocene oxamidide complexes prompted kinetic measurements

dx.doi.org/10.1021/ja208562d | J. Am. Chem.Soc. 2012, 134, 3377−3386

of the C−C bond forming reaction. Because the half-life for the conversion of **Int** to the isomers of **2** is on the order of minutes at 23 °C, the rates of the reaction were conveniently measured by ^{1}H NMR spectroscopy. In a typical experiment, a 0.026 M solution of **1** in benzene-d_6 was treated with 4 atm of carbon monoxide and the conversion of reactants to products was measured over time. Plots of concentration versus time follow a first-order rate equation and representative examples are presented in Figure S2 in the Supporting Information. We note that the observed rate constants represent the disappearance of **Int**; the partial precipitation of **2-C$_1$** and **2-C$_2$** does not permit reliable integrations and prohibits reliable determination of rate constants based on the appearance of the product.

The activation parameters for the conversion of **Int** to **2** were determined by measuring rate constants for the reaction over a 30 degree temperature range (Figure 6). Unfortunately the high

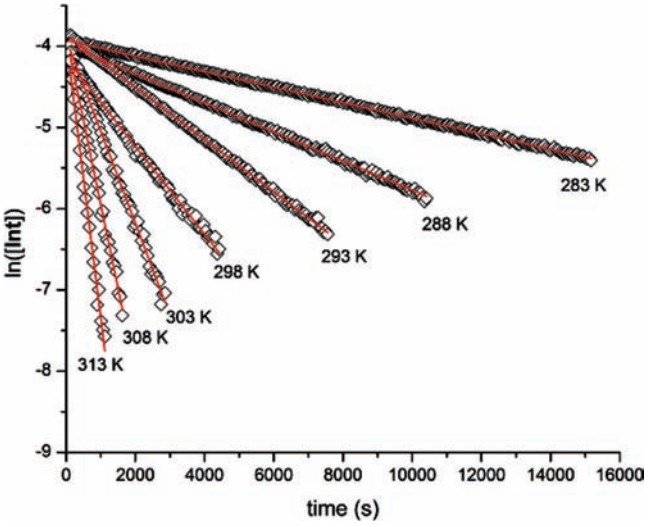

Figure 6. First-order plots for the disappearance of **Int** as a function of time at various temperatures.

reactivity and instability of **2** prohibited measurement of rate constants over a wider temperature window. An Eyring plot (Figure 7) was constructed from these limited data (Table S1), and activation parameters of $\Delta H^{\ddagger}$ = 20.5(3) kcal/mol and $\Delta S^{\ddagger}$ = −4.4(8) eu were extracted. The entropy of activation is consistent with a unimolecular process and given the narrow temperature range should be interpreted cautiously.

Because 1 equiv of carbon monoxide is lost upon conversion of **Int** to the isomers of **2**, the dependence of the reaction rate on CO concentration was studied. Reactions were carried out in the absence of added gas and at 1 and 4 atm of carbon monoxide at 20 °C. The observed rate constants determined from these experiments are reported in Table 1. The small variance within the rate constants suggests no overall inhibition by added carbon monoxide. More careful inspection of the data (see insert Figure 8) for the reaction carried out in the absence of CO revealed nonlinear behavior due to a faster reaction at early times (t = 0 to 5 min) that then converges to linearity and at a decreased rate. This increased initial rate also coincides with the formation of **2-C$_1$** (as observed by ^{1}H NMR spectroscopy), which eventually is suppressed as **2-C$_2$** becomes the dominant product of the reaction. Thus, the nonlinear behavior is a consequence of formation of the C_1 isomer at low

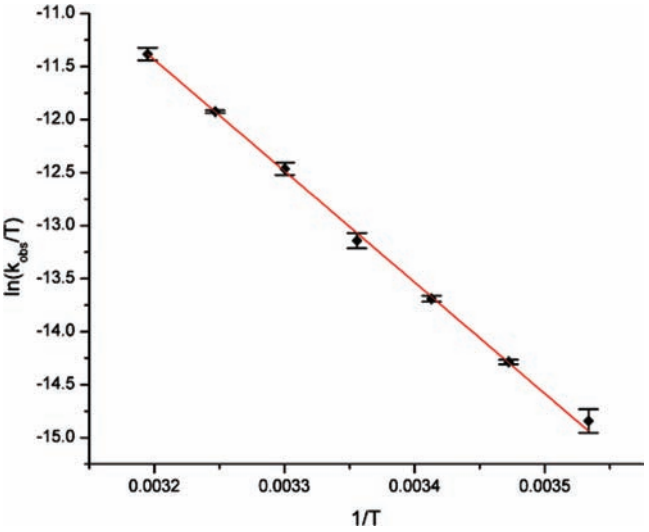

Figure 7. Eyring plot for the conversion of **Int** to **2**.

Table 1. Observed Rate Constants for the Conversion of Int to 2 as a Function of Added CO at 20 °C

Amount of CO	$k_{obs} \times 10^4$ (s^{-1})
4 atm	3.32(9)
1 atm	3.52(16)
0 atm	3.75(20)

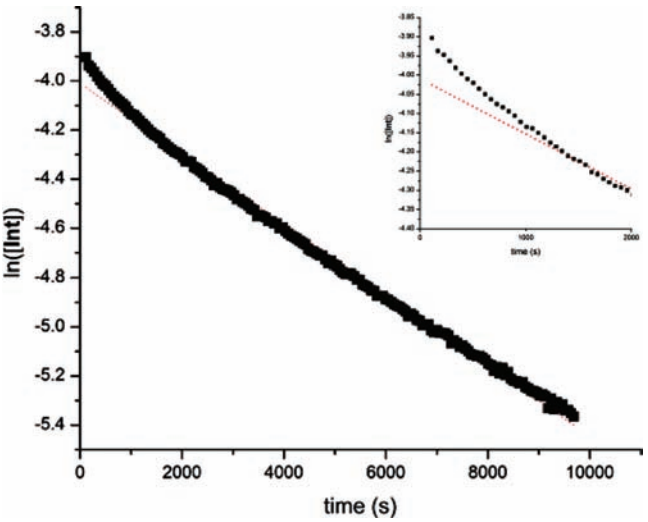

Figure 8. Plot of the conversion of **Int** to **2** as a function of time at 20 °C. Inset highlights the deviation from linearity at early reaction times.

CO pressures, which then converts to a regime where the C_2 compound becomes competitive due to the build up of carbon monoxide from dissociation from **Int**. These observations suggest that the pathways to **2-C$_1$** and **2-C$_2$** diverge at **Int** and that formation of **2-C$_1$** is faster than **2-C$_2$**. In addition, the terminal CO ligand in **Int** is also important in determining the stereochemical outcome of the reaction.

Proposed Mechanism. The structural elucidation of **2-C$_1$**, observation and characterization of **Int**, subsequent ^{13}C labeling, and kinetic studies provide experimental insight into the mechanism of hafnocene oxamidide formation. Previous work from our laboratory has provided experimental evidence for the formation of an intermediate μ-nitrido hafnocene

dx.doi.org/10.1021/ja208562d | J. Am. Chem.Soc. 2012, 134, 3377−3386

Scheme 4. Proposed Mechanism for the Conversion of Int to 2-C_1 and 2-C_2

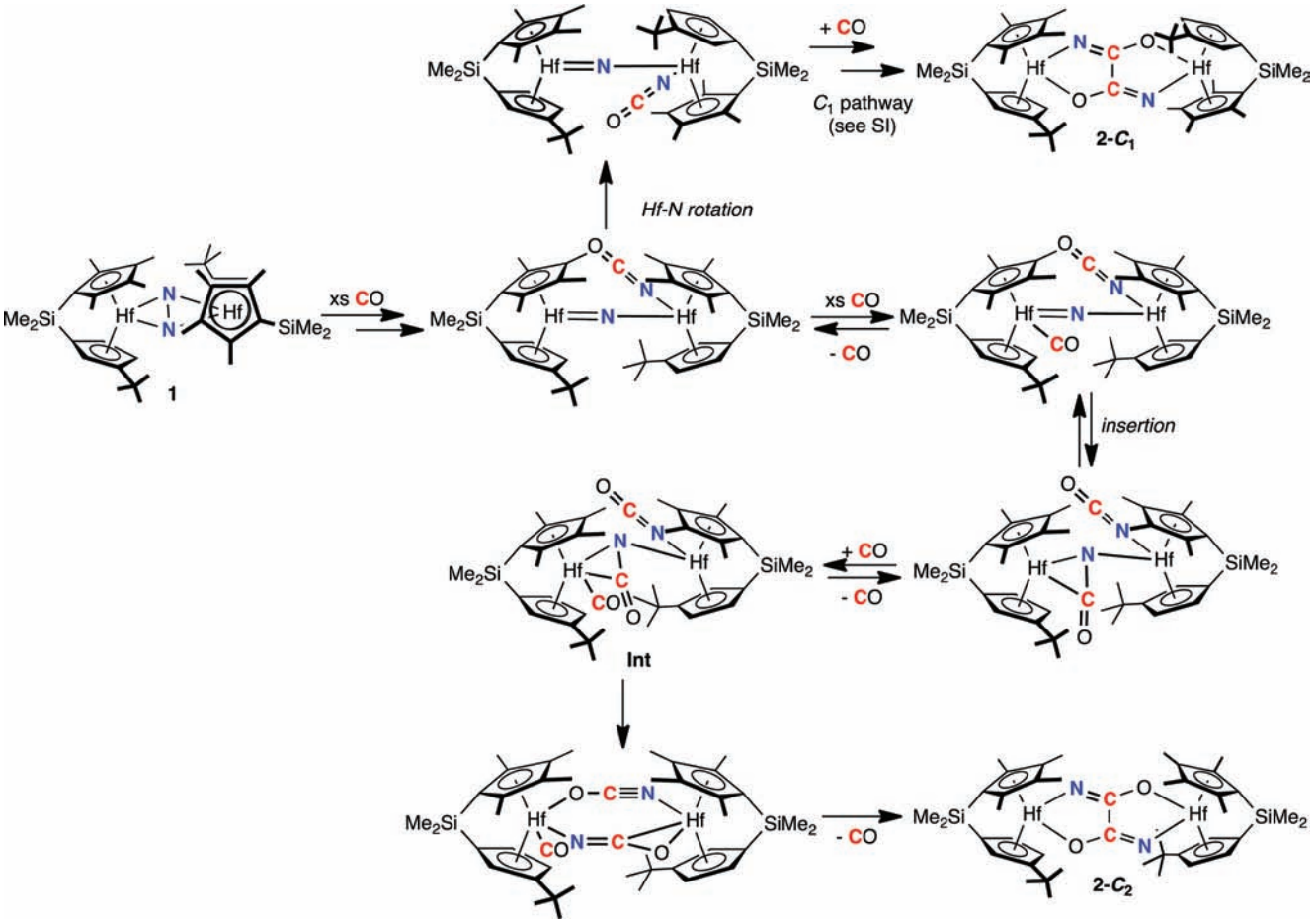

isocyanate complex following addition of 1 equiv of carbon monoxide.[12] Subsequent computational studies supported a pathway involving initial CO insertion into a Hf–N bond followed by retro [2 + 2] cycloaddition to form the putative μ-nitrido compound.[17] Therefore, mechanisms accounting for hafnocene oxamidide formation will likely proceed through this species.

Based on the experimental data, a mechanism for hafnocene oxamidide formation is presented in Scheme 4. Coordination of carbon monoxide to the μ-nitrido hafnocene isocyanate intermediate precedes insertion into the Hf–N bond to form the bridging isocyanate complex. Capture of this compound by excess carbon monoxide furnishes the observed intermediate, **Int**. The stereochemistry of the unobserved compounds is speculative, but the preferred structures presented in Scheme 4 are believed to be the most reasonable based on the reaction outcome.

The influence of the CO pressure on the rate of conversion of **Int** to the hafnocene oxamidide products provides insight into the relative rates of C–C coupling. The kinetic data support more rapid formation of the C_1 isomer that is suppressed by a slower process at higher CO pressures to form the C_2 product. The CO is either added as a reagent or formed during the course of the reaction from dissociation from **Int**. This behavior also accounts for the observation of a sole isomer of **Int** and establishes the compound as an essential intermediate, and not just an observable side product, in hafnocene oxamidide formation.

The lack of CO inhibition on the rate of conversion of **Int** to the hafnocene oxamidides suggests that the terminal carbonyl ligand remains coordinated to the metal during rate determining C–C bond formation. However, the isotopic labeling experiments demonstrate that the terminal CO ligand is labile and bridging isocyanate formation is reversible. Thus all steps leading to the carbonyl adduct of the μ-nitrido hafnocene are also reversible. Carbon–carbon bond formation occurs via coupling of the terminal and bridging isocyanates with concurrent displacement of the terminal carbonyl ligand. This mechanism deviates from the computational work reported by Schwarz as the experimental data for the presence of the terminal CO ligand was not available. However, our current experimental studies suggest that the computational studies should be reevaluated with the terminal CO ligand present.

Reactivity of the Intermediate: CO Homologation. The incorporation of three molecules of carbon monoxide in the structure of **Int** raised the question of whether these carbon equivalents could be used productively and additional C–C bond formation could be observed upon addition of the appropriate reagents.[22,23] Addition of 5 equiv of CH_3I to a benzene-d_6 solution of **Int** resulted in clean and rapid conversion to a new C_1 symmetric dihafnocene complex, **4** (eq 1).

The solid state structure of **4** was determined by X-ray diffraction and confirms retention of three molecules of CO in the compound along with formal 1,2-addition of CH_3I across the Hf–N bond of **Int** (Figure 9; see Table 2 for bond/angle

dx.doi.org/10.1021/ja208562d | J. Am. Chem.Soc. 2012, 134, 3377–3386

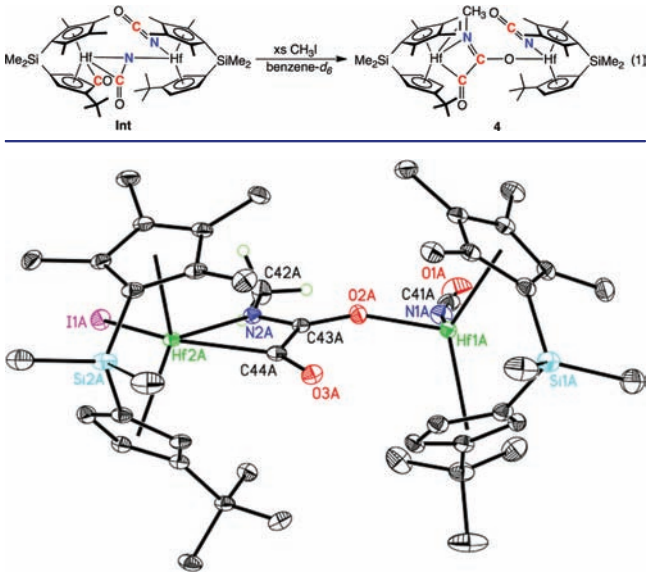

Figure 9. Solid state molecular structure of the (*S*, *S*) enantiomer of **4** at 30% probability ellipsoids. Hydrogen atoms, except those bonded to C(42A), omitted for clarity.

Table 2. Selected Metrical Parameters for 4

Bond/Angle	Distance (Å)/Angle (deg)
Hf(1A)−O(3A)	1.9747(14)
Hf(1A)−N(1A)	2.1035(19)
Hf(2A)−O(3A)	1.9647(14)
Hf(2A)−N(2A)	2.1034(18)
Hf(1A)−O(3A)−Hf(2A)	175.91(8)
N(1A)−C(41A)−O(1A)	178.6(3)
N(2A)−C(42A)−O(2A)	179.0(4)

parameters). Migration of the bridging isocyanate ligand from *C*, *N* bound to *N*, *C* (from CO insertion), to *O* bound accompanies nitrogen methylation and imidate formation. The stereochemistry of **4** has the like cyclopentadienyl rings oriented *cisoid* across the bimetallic structure and in a *syn* arrangement yet geared to avoid steric interactions. For the hafnocene bearing the iodide ligand, the halide is directed away from the *tert*-butyl substituent and the carbonyl derived from the former terminal CO ligand is *syn* to the [^{t}Bu]. The other hafnocene subunit has two ligands in the metallocene wedge: the [NCO] *syn* to the ^{t}Bu group and the oxygen from the imidate ligand.

Natural abundance and ^{13}C, ^{15}N isotopologues of **4** were also characterized by multinuclear NMR spectroscopy. The benzene-d_6 {^{1}H}^{13}C NMR spectrum of **4**-$^{13}\mathbf{C}_3{}^{15}\mathbf{N}_2$ is presented in the top portion of Figure 10. A diagnostic doublet ($^1J_{C-N}$ = 32.9 Hz) was located at 135.77 ppm and is assigned as the terminal isocyanate ligand. For the more unusual bridging imidate ligand, two multiplets are observed at 178.89 and 291.24 ppm. The more upfield resonance exhibits coupling to both ^{13}C ($^1J_{C-C}$ = 13.8 Hz) and ^{15}N ($^1J_{C-N}$ = 6.6 Hz) and is assigned as the carbon bound directly to the nitrogen. The more downfield multiplet also couples to both nuclei ($^2J_{C-N}$ = 11.9 Hz) and is assigned as the acyl carbon based on chemical shift despite having the larger coupling to ^{15}N. Accordingly, the ^{15}N NMR spectrum exhibits two resonances: a doublet at 91.4 ppm ($^1J_{C-N}$ = 32.9 Hz) for the terminal isocyanate and a

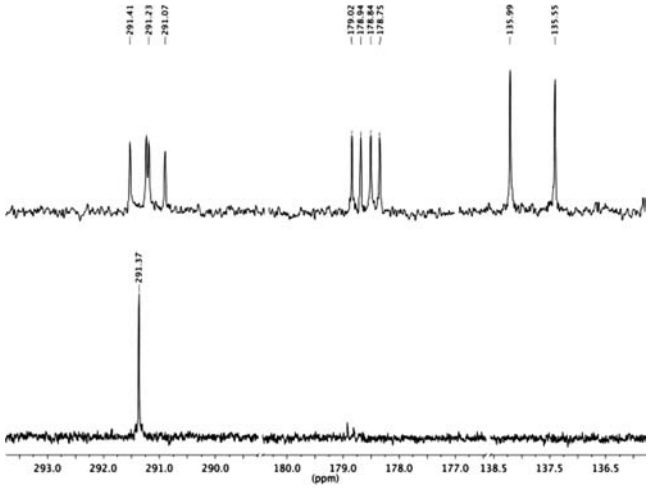

Figure 10. Benzene-d_6 {^{1}H}^{13}C NMR spectrum of **4**-$^{13}\mathbf{C}_3{}^{15}\mathbf{N}_2$ (top) and **4**-$^{13}\mathbf{C}_1$ (bottom).

multiplet at 227.3 ppm ($^2J_{C-N}$ = 11.9 Hz; $^1J_{C-N}$ = 6.6 Hz) for the nitrogen in the imidate.

To provide additional support for the ^{13}C NMR assignments for the imidate ligand, a ^{13}C isotopic labeling experiment was conducted. The isotopologue of **Int**-$^{13}\mathbf{C}$ was prepared with only the terminal carbonyl ^{13}C labeled. A benzene-d_6 solution of this compound was treated with methyl iodide, and the ^{13}C NMR spectrum was recorded. As is presented in the bottom portion of Figure 10, only the most downfield resonance at 291.37 ppm is ^{13}C labeled, providing additional support for the assignment as the acyl resonance. Isotopic exchange into this site was also supported by infrared spectroscopy. The solid state spectrum (KBr) of the ^{13}C labeled compound exhibits a band at 1541 cm^{-1}, shifted from the value observed at 1605 cm^{-1} in the natural abundance material.

The reactivity of **Int** with the heterocumulenes ^{t}BuNCO and CO_2 was also explored. Addition of 1 equiv of *tert*-butyl isocyanate to a benzene-d_6 solution of **Int** furnished a new C_1 symmetric hafnocene product identified as **5**, arising from C−C coupling and cycloaddition of the heterocumulene across the Hf−N bond (eq 2). It is notable that both 1,2-addition of a

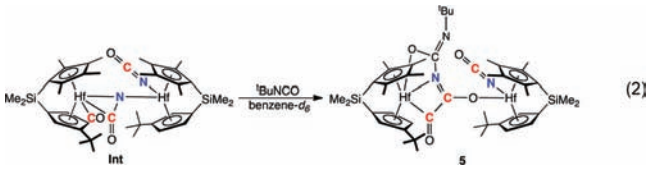

C−X bond and cycloaddition of a heterocumulene trap the CO insertion product.

Multinuclear NMR spectroscopy and isotopic labeling experiments were used to confirm ^{t}BuNCO cycloaddition and N−C and C−C bond formation. The benzene-d_6 {^{1}H}^{13}C NMR spectrum of **5**-$^{13}\mathbf{C}_2{}^{15}\mathbf{N}_2$ prepared from **Int**-$^{13}\mathbf{C}_2{}^{15}\mathbf{N}_2$ is presented in Figure 11 and confirms N−C and C−C bond formation. In addition to the terminal [NCO] doublet ($^1J_{N-C}$= 33.9 Hz), doublet of doublet resonances centered at 176.15 and 303.60 were observed, corresponding to the N-bound carbon and the Hf-bound carbon, respectively. The stereochemistry of the preferred and observed isomer of **5** is unknown in the absence of crystallographic data; however, it is likely the structure is similar to **4** with the hafnium acyl groups and the

dx.doi.org/10.1021/ja208562d | *J. Am. Chem.Soc.* 2012, 134, 3377−3386

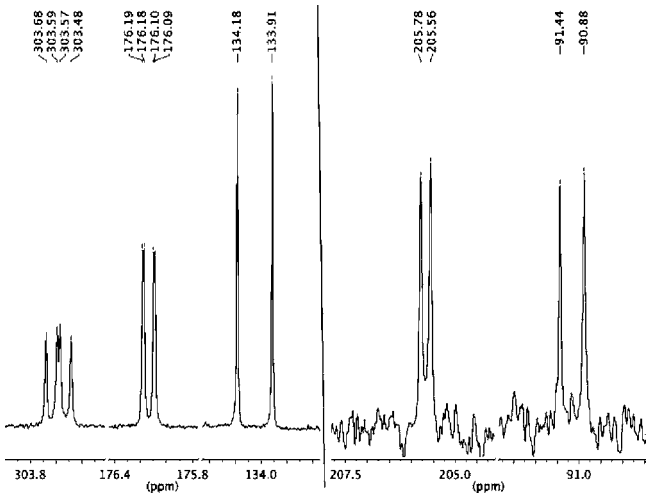

Figure 11. Benzene-d_6 $\{^1H\}^{13}C$ NMR (left) and ^{15}N NMR (right) spectra of **5**-$^{13}C_2N_2$.

terminal isocyanate *syn* to the *tert*-butyl groups on the cyclopentadienyl ligands.

The reaction with carbon dioxide produced a notably different outcome. Treatment of a benzene-d_6 solution of **Int** with 1.5 equiv of CO_2 did not produce a C_1 symmetric compound as was observed with MeI and ^{t}BuNCO but rather a C_2 symmetric product identified as the μ-oxo dihafnocene bis(isocyanate) **6** with the loss of 2 equiv of carbon monoxide (eq 3).

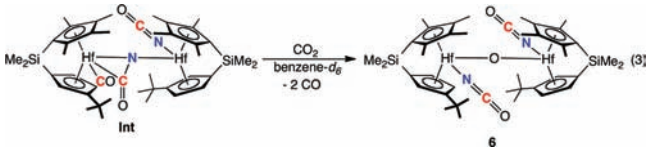

The structure of **6** was established by multinuclear NMR spectroscopy and X-ray diffraction. The solid state structure of the (*S*, *S*) enantiomer is presented in Figure 12 and establishes

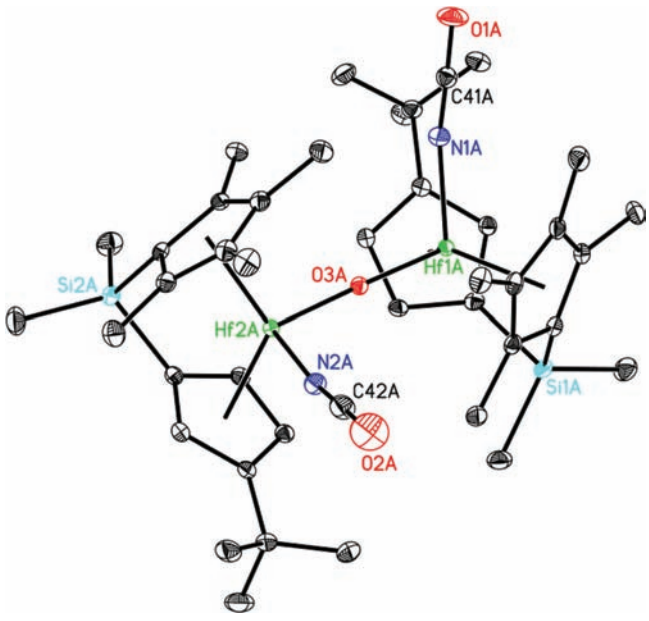

Figure 12. Solid state molecular structure of the (*S*, *S*) enantiomer of **6** at 30% probability ellipsoids. Hydrogen atoms omitted for clarity.

the presence of two terminal isocyanate ligands and a bridging oxo. The Hf−O−Hf angle is nearly linear (175.91(8)°) and preserves the C_2 symmetry of the compound. In the observed isomer, each of the terminal isocyanate ligands is directed over the *tert*-butyl substituents of the cyclopentadienyl rings.

The benzene-d_6 ^{13}C NMR spectrum of **6**-$^{13}C_2^{15}N_2$ exhibits a single resonance centered at 94.6 ppm with appropriate coupling ($^1J_{C-N}$ = 33.8 Hz) for a terminal isocyanate. To determine the origin of the terminal isocyanate carbons, an isotopic labeling experiment was conducted. Treatment of **Int**-$^{15}N_2$ with $^{13}CO_2$ followed by analysis by ^{15}N NMR spectroscopy (Figure S5) revealed an approximately 1:1 ratio of [$^{15}N^{13}CO$] and [^{15}NCO] ligands consistent with the formation of one isocyanate from carbon *monoxide* and the other from carbon *dioxide*. These results, coupled with the loss of two molecules of CO from **Int**, are also consistent with the bridging oxo ligand being derived from CO_2 deoxygenation.

CONCLUSIONS

Investigations into the mechanism of CO-induced N_2 bond cleavage with a hafnocene dinitrogen complex to form the corresponding oxamidide compound have been carried out. An intermediate dihafnocene compound bearing terminal and bridging isocyanates and a terminal carbonyl ligand was detected by monitoring the low temperature carbonylation by multinuclear NMR spectroscopy. The observation of this species, coupled with previously reported reactivity and computational studies, established rapid N−N bond cleavage and rate determining C−C bond formation via isocyanate coupling to form the oxamidide. Kinetic data support the presence of the terminal CO ligand in the C−C bond forming step and more rapid conversion to the C_1 rather than C_2 symmetric product. The structure of the former hafnocene oxamidide product has been elusive but since definitively characterized in this study. Isotopic labeling experiments established the lability of the terminal CO ligand as well as the reversibility of N−C bond formation in the bridging [NCO] moiety. Additional C−C bond formation by CO homologation was achieved by 1,2-addition of methyl iodide or by cycloaddition of ^{t}BuNCO across the Hf−N bond. Deoxygenation of carbon dioxide was also found to be another route to N−C bond formation from cleaved dinitrogen to yield terminal hafnocene isocyanate complexes.

EXPERIMENTAL SECTION

Preparation of ([Me$_2$Si(η^5-C$_5$Me$_4$)(η^5-C$_5$H$_3$-3-^{t}Bu)]Hf)$_2$(μ-NCO)-(CO)(NCO) (Int). In a drybox, a J. Young NMR tube was charged with 0.020 g (0.020 mmol) of **1** and approximately 0.6 mL of benzene-d_6 were added. On a high vacuum line, the vessel was degassed and 4 atm of carbon monoxide were added at −196 °C. The contents of the vessel were thawed and shaken for 20 s until the solution turned red-brown and clear, signaling the formation of **Int**. The tube was placed in an ice bath, and the solvent was lyophilized on the high vacuum line. The tube was transferred to the glovebox, and the solid was transferred to a vial for storage. Anal. Calcd for $C_{43}H_{60}O_3N_2Si_2Hf_2$: C, 48.44; H, 5.67; N, 2.63. Found: C, 48.17; H, 5.87; N, 2.27. ^1H NMR (benzene-d_6): δ = 0.44s, 3H, SiMe_2), 0.52 (s, 3H, SiMe_2), 0.57 (s, 3H, SiMe_2), 0.63 (s, 3H, SiMe_2), 1.28 (s, 9H, C$_5$H$_3$CMe_3), 1.50 (s, 3H, C$_5Me_4$), 1.51 (s, 9H, C$_5$H$_3$CMe_3), 1.85 (s, 3H, C$_5Me_4$), 1.86 (s, 3H, C$_5Me_4$), 1.94 (s, 3H, C$_5Me_4$), 2.05 (s, 3H, C$_5Me_4$), 2.13 (s, 3H, C$_5Me_4$), 2.30 (s, 3H, C$_5Me_4$), 2.33 (s, 3H, C$_5Me_4$), 5.17 (m, 1H, C$_5H_3$CMe$_3$), 5.47 (m, 1H, C$_5H_3$CMe$_3$), 5.61 (m, 1H, C$_5H_3$CMe$_3$), 5.83 (m, 1H, C$_5H_3$CMe$_3$), 5.93 (m, 1H, C$_5H_3$CMe$_3$), 7.14 (m, 1H, C$_5H_3$CMe$_3$). ^1H NMR (toluene-d_8): δ = 0.45 (s, 3H, SiMe_2), 0.55 (s, 3H, SiMe_2), 0.59 (s, 3H, SiMe_2), 0.64 (s, 3H, SiMe_2), 1.24 (s, 9H, C$_5$H$_3$CMe_3), 1.42 (s, 3H, C$_5Me_4$),

dx.doi.org/10.1021/ja208562d | J. Am. Chem.Soc. 2012, 134, 3377−3386

1.46 (s, 9H, $C_5H_3CMe_3$), 1.82 (s, 3H, C_5Me_4), 1.86 (s, 3H, C_5Me_4), 1.93 (s, 3H, C_5Me_4), 2.02 (s, 3H, C_5Me_4), 2.10 (s, 3H, C_5Me_4), 2.24 (s, 3H, C_5Me_4), 2.28 (s, 3H, C_5Me_4), 5.12 (m, 1H, $C_5H_3CMe_3$), 5.43 (m, 1H, $C_5H_3CMe_3$), 5.51 (m, 1H, $C_5H_3CMe_3$), 5.71 (m, 1H, $C_5H_3CMe_3$), 5.82 (m, 1H, $C_5H_3CMe_3$), 7.06 (m, 1H, $C_5H_3CMe_3$). $\{^1H\}^{13}C$ NMR (toluene-d_8): δ = −0.81 ($SiMe_2$), −0.48 ($SiMe_2$), −0.06 ($SiMe_2$), 0.11 ($SiMe_2$), 11.13 (Cp*Me*), 11.27 (Cp*Me*), 11.72 (Cp*Me*), 13.88 (Cp*Me*), 14.00 (Cp*Me*), 14.13 (Cp*Me*), 14.31 (Cp*Me*), 14.60 (Cp*Me*), 30.78 (CMe_3), 32.13 (CMe_3), 33.06 (CMe_3), 33.38 (CMe_3), 90.94, 97.30, 98.26, 99.53, 107.52, 107.89, 112.12, 114.71, 115.17, 115.26, 117.68, 117.88, 118.23, 118.73, 123.89, 127.05, 128.18, 129.08, 132.28, 152.61 (*Cp*), 134.48 (NCO, $^1J_{CN}$ = 32.9 Hz), 192.50 (μ-NCO, $^1J_{CN}$ = 9.6 Hz, $^2J_{CC}$ = 13.7 Hz), 247.07 (Hf-CO, $^2J_{CC}$ = 13.7 Hz). ^{15}N NMR (toluene-d_8): δ = 89.60 (^{15}NCO, $^1J_{CN}$ = 32.9 Hz), 241.14 (μ-^{15}NCO, $^1J_{CN}$ = 9.6 Hz). IR (KBr): ν = 2220 cm^{-1} (NCO); ν = 1959 cm^{-1} (CO); ν = 1914 (^{13}CO); ν = 1588 cm^{-1} (μ-NCO).

Preparation of ([$Me_2Si(\eta^5$-$C_5Me_4)(\eta^5$-C_5H_3-3-^{t}Bu)]Hf)$_2$((NCH$_3$)-C_2O_2)(I)(NCO) (4). In a drybox, a J. Young NMR tube was charged with 0.020 g (0.020 mmol) of **1** and approximately 0.6 mL of benzene-d_6 were added. On a high vacuum line, the vessel was degassed and 4 atm of carbon monoxide were added at −196 °C. The contents of the vessel were thawed and shaken for 20 s until the solution turned red-brown and clear, signaling the formation of **Int**. The tube was degassed, and 0.100 mmol of CH_3I was admitted via a calibrated gas bulb. The tube was thawed and shaken, and complete conversion to **4** after several minutes was confirmed by NMR spectroscopy. The solvent was evacuated, and the remaining red oil was washed with pentane furnishing pure **4** in 61% yield (from 3 combined batches). Anal. Calcd for $C_{44}H_{63}Hf_2IN_2O_3Si_2$: C, 43.75; H, 5.26; N, 2.32. Found: C, 43.53; H, 5.20; N, 2.02. ^1H NMR (benzene-d_6): δ = 0.41 (s, 3H, $SiMe_2$), 0.48 (s, 3H, $SiMe_2$), 0.53 (s, 3H, $SiMe_2$), 0.64 (s, 3H, $SiMe_2$), 1.23 (s, 9H, $C_5H_3CMe_3$), 1.42 (s, 9H, $C_5H_3CMe_3$), 1.49 (s, 3H, C_5Me_4), 1.65 (s, 3H, C_5Me_4), 1.76 (s, 3H, C_5Me_4), 1.89 (s, 6H, C_5Me_4, 2 coincident), 2.06 (s, 3H, C_5Me_4), 2.29 (s, 3H, C_5Me_4), 2.49 (s, 3H, C_5Me_4), 3.37 (s, 3H, N−CH_3, $^1J_{CH}$ = 137.8 Hz, $^2J_{NH}$ = 1.5 Hz), 5.27 (m, 1H, $C_5H_3CMe_3$), 5.33 (m, 1H, $C_5H_3CMe_3$), 5.96 (m, 1H, $C_5H_3CMe_3$), 6.18 (m, 1H, $C_5H_3CMe_3$), 6.24 (m, 1H, $C_5H_3CMe_3$), 7.54 (m, 1H, $C_5H_3CMe_3$). $\{^1H\}^{13}C$ NMR (benzene-d_6): δ = −1.26 ($SiMe_2$), −0.99 ($SiMe_2$), 0.58 ($SiMe_2$), 1.00 ($SiMe_2$), 11.30 (Cp*Me*), 11.99 (Cp*Me*), 12.25 (Cp*Me*), 14.64 (Cp*Me*), 14.89 (Cp*Me*), 15.91 (Cp*Me*), 17.00 (Cp*Me*), 30.83 (CMe_3), 31.22 (CMe_3), 32.70 (CMe_3), 33.71 (CMe_3), 38.83 (N-CH_3, $^1J_{CN}$ = 3.0 Hz, $^2J_{CC}$ = 6.2 Hz, $^3J_{CC}$ = 3.2 Hz) 100.11, 100.36, 105.26, 107.10, 109.27, 110.72, 111.84, 113.99, 114.56, 116.30, 116.53, 119.98, 123.51, 125.60, 126.03, 127.60, 127.80, 129.67, 130.66, 156.47 (*Cp*), 135.77 (NCO, $^1J_{CN}$ = 32.9 Hz), 178.89 (Hf—(C═O)—C═N, $^1J_{CC}$ = 13.8 Hz, $^1J_{CN}$ = 6.6 Hz, $^2J_{CC}$ = 3.2 Hz), 291.24 (Hf—(*C*═O)—C═N, $^1J_{CC}$ = 13.8 Hz, $^2J_{CN}$ = 11.9 Hz, $^3J_{CC}$ = 6.2 Hz), one Cp*Me* resonance not located. ^{15}N NMR (benzene-d_6): δ = 91.4 (^{15}NCO), 227.3 (^{15}N-CH_3). IR (KBr): ν = 2218 cm^{-1} (NCO); ν = 1605 cm^{-1} (Hf—C═O).

Preparation of ([$Me_2Si(\eta^5$-$C_5Me_4)(\eta^5$-C_5H_3-3-^{t}Bu)]Hf)$_2$-((N(^{t}BuNCO))C_2O_2)(NCO) (5). The hafnocene intermediate, **Int**, was generated as described above with 0.020 g (0.020 mmol) of **1**. Following preparation of **Int**, the NMR tube was degassed and 0.100 mmol of *tert*-butylisocyanate was admitted *via* a calibrated gas bulb. The tube was thawed and shaken, and complete conversion to **5** after several minutes was confirmed by NMR spectroscopy. The solvent was evacuated, and the remaining brown oil was washed with pentane furnishing pure **5** in 40% yield (from 3 combined batches). Anal. Calcd for $C_{48}H_{69}Hf_2N_3O_4Si_2$: C, 49.48; H, 5.97; N, 3.61. Found: C, 49.28; H, 5.75; N, 3.26. ^1H NMR (benzene-d_6): δ = 0.44s, 3H, $SiMe_2$), 0.48 (s, 3H, $SiMe_2$), 0.54 (s, 6H, $SiMe_2$, 2 coincident), 1.26 (s, 9H, $C_5H_3CMe_3$), 1.43 (s, 9H, $C_5H_3CMe_3$), 1.52 (s, 9H, C═NCMe_3), 1.56 (s, 3H, C_5Me_4), 1.62 (s, 3H, C_5Me_4), 1.68 (s, 3H, C_5Me_4), 2.03 (s, 3H, C_5Me_4), 2.05 (s, 3H, C_5Me_4), 2.16 (s, 3H, C_5Me_4), 2.18 (s, 3H, C_5Me_4), 2.20 (s, 3H, C_5Me_4), 5.57 (m, 1H, $C_5H_3CMe_3$), 5.59 (m, 1H, $C_5H_3CMe_3$), 5.63 (m, 1H, $C_5H_3CMe_3$), 5.91 (m, 1H, $C_5H_3CMe_3$), 6.36 (m, 1H, $C_5H_3CMe_3$), 6.51 (m, 1H, $C_5H_3CMe_3$). $\{^1H\}^{13}C$ NMR (benzene-d_6): δ = −0.87 ($SiMe_2$), −0.51 ($SiMe_2$), 0.11 ($SiMe_2$), 0.63 ($SiMe_2$), 12.69 (Cp*Me*), 12.78 (Cp*Me*), 12.97 (Cp*Me*), 14.63 (Cp*Me*), 14.89 (Cp*Me*), 14.99 (Cp*Me*), 15.36 (Cp*Me*), 15.72 (Cp*Me*), 31.92 (CMe_3), 32.19 (CMe_3), 32.93 (N−CMe_3), 33.46 (CMe_3), 34.18 (CMe_3), 106.75, 107.07, 108.20, 108.47, 110.62, 110.93, 111.72, 112.57, 114.80, 116.93, 119.13, 121.22, 122.57, 123.52, 124.48, 125.94, 127.80, 129.66, 150.28, 151.68 (*Cp*), 134.07 (NCO, $^1J_{CN}$ = 33.9 Hz), 176.15 (Hf—(C═O)—C═N, $^1J_{CC}$ = 10.9 Hz, $^1J_{CN}$ = 1.3 Hz), 303.60 (Hf—(C═O)—C═N, $^1J_{CC}$ = 10.9 Hz, $^2J_{CN}$ = 13.8 Hz). ^{15}N NMR (benzene-d_6): δ = 91.1 (^{15}NCO, $^1J_{NC}$ = 33.9 Hz), 205.7 (Hf—(CO)—C═^{15}N, $^2J_{CN}$ = 13.8 Hz, $^1J_{CN}$ = 1.3 Hz).

Preparation of ([$Me_2Si(\eta^5$-$C_5Me_4)(\eta^5$-C_5H_3-3-^{t}Bu)]Hf)$_2(\mu$-O)-(NCO)$_2$ (6). The hafnocene intermediate, **Int**, was generated as described above with 0.020 g (0.020 mmol) of **1**. Following preparation of **Int**, the NMR tube was charged with 0.03 mmol of carbon dioxide *via* a calibrated gas bulb. The tube was thawed and shaken, and complete conversion to **6** was confirmed by NMR spectroscopy. The solvent was evacuated, and the remaining brown oil was washed with pentane furnishing pure **6** in 56% yield (from 3 combined batches). Anal. Calcd for $C_{42}H_{60}O_3N_2Si_2Hf_2$: C, 47.85; H, 5.74; N, 2.66. Found: C, 47.58; H, 5.55; N, 2.38. ^1H NMR (benzene-d_6): δ = 0.51 (s, 3H, $SiMe_2$), 0.60 (s, 3H, $SiMe_2$), 1.40 (s, 9H, $C_5H_3CMe_3$), 1.93 (s, 3H, C_5Me_4), 1.97 (s, 3H, C_5Me_4), 2.00 (s, 3H, C_5Me_4), 2.12 (s, 3H, C_5Me_4), 5.47 (m, 1H, $C_5H_3CMe_3$), 5.99 (m, 1H, $C_5H_3CMe_3$), 6.57 (m, 1H, $C_5H_3CMe_3$). $\{^1H\}^{13}C$ NMR (benzene-d_6): δ = −0.34 ($SiMe_2$), 0.27 ($SiMe_2$), 11.84 (Cp*Me*), 12.20 (Cp*Me*), 14.42 (Cp*Me*), 14.96 (Cp*Me*), 31.30 (CMe_3), 32.32 (CMe_3), *Cp* resonances not located. 135.76 (NCO, $^1J_{CN}$ = 33.8 Hz). ^{15}N NMR (benzene-d_6): δ = 94.6 (^{15}NCO, $^1J_{CN}$ = 33.8 Hz). IR (KBr): ν = 2222 cm^{-1} (NCO).

■ ASSOCIATED CONTENT

Ⓢ Supporting Information

General experimental considerations, additional spectral data, crystallographic data for **2-C$_2$**, **2-C$_1$-(^{t}BuNCO)$_2$**, **4**, and **6**. This material is available free of charge via the Internet at http://pubs.acs.org.

■ AUTHOR INFORMATION

Corresponding Author

pchirik@princeton.edu

Notes

The authors declare no competing financial interest.

■ ACKNOWLEDGMENTS

We thank the Director of the Office of Basic Energy Sciences, Chemical Sciences Division, U.S. Department of Energy (DE-FG-02-05ER15659) for financial support. S.P.S. thanks the Natural Sciences and Engineering Research Council of Canada for a predoctoral fellowship (PGS-D).

■ REFERENCES

(1) (a) Hidai, M.; Mizobe, Y. *Chem. Rev.* **1995**, *95*, 1115. (b) Hidai, M. *Coord. Chem. Rev.* **1999**, *185−186*, 99. (c) Shaver, M. P.; Fryzuk, M. D. *Adv. Synth. Catal.* **2003**, *345*, 1061. (d) Ertl, G. *Angew. Chem., Int. Ed.* **2008**, *47*, 3524. (e) Hazari, N. *Chem. Soc. Rev.* **2010**, *39*, 4044.

(2) (a) Ertl, G. *Angew. Chem.* **2008**, *120*, 3578. (b) Erisman, J. W.; Sutton, M. A.; Galloway, J.; Klimont, Z.; Winiwarter, W. *Nat. Geosci.* **2008**, *1*, 636.

(3) (a) Burgess, B. K.; Lowe, D. J. *Chem. Rev.* **1996**, *96*, 2983. (b) Rees, D. C.; Tezcan, F. A.; Haynes, C. A.; Walton, M. Y.; Andrade, S.; Einsle, O.; Howard, J. B. *Philos. Trans. R. Soc. London, Ser. A* **2005**, *363*, 971.

(4) (a) Li, J.; Li, S. H. *Angew. Chem., Int. Ed.* **2008**, *47*, 8040. (b) Chirik, P. J. *Dalton Trans.* **2007**, 16. (c) Himmel, H. J.; Hubner, O.; Klopper, W.; Manceron, L. *Angew. Chem.* **2006**, *45*, 2799. (d) Hendrich, M. P.; Gunderson, W.; Behan, R. K.; Green, M. T.;

Mehn, M. P.; Betley, T. A.; Lu, C. C.; Peters, J. C. *Proc. Natl. Acad. Sci. U.S.A.* **2006**, *103*, 17107.
(5) (a) Laplaza, C. E.; Cummins, C. C. *Science* **1998**, *268*, 861. (b) Laplaza, C. E.; Johnson, M. J. A.; Peters, J. C.; Odom, A. L.; Kim, E.; Cummins, C. C.; George, G. N.; Pickering, I. J. *J. Am. Chem. Soc.* **1996**, *118*, 8623. (c) Cui, Q.; Musaev, D. G.; Svennson, M.; Sieber, S.; Morokuma, K. *J. Am. Chem. Soc.* **1995**, *117*, 12366.
(6) (a) Akagi, F.; Matsuo, T.; Kawaguchi, H. *Angew. Chem., Int. Ed.* **2007**, *46*, 8778. (b) Tanaka, H.; Shiota, Y.; Matsuo, T.; Kawaguchi, H.; Yoshizawa, K. *Inorg. Chem.* **2009**, *48*, 3875.
(7) Chatt, J.; Dilworth, J. R.; Richards, R. L. *Chem. Rev.* **1965**, *78*, 589.
(8) (a) Yandulov, D. V.; Schrock, R. R. *Science* **2003**, *301*, 76. (b) Schrock, R. R. *Chem. Commun.* **2003**, 2389. (c) Schrock, R. R. *Acc. Chem. Res.* **2005**, *38*, 955. (d) Neese, F. *Angew. Chem., Int. Ed.* **2006**, *45*, 196.
(9) Arashiba, K.; Miyake, Y.; Nishibayashi, Y. *Nat. Chem.* **2011**, *3*, 120.
(10) (a) Fryzuk, M. D.; Love, J. B.; Rettig, S. J.; Young, V. G. *Science* **1997**, *275*, 1445. (b) Pool, J. A.; Lobkovsky, E.; Chirik, P. J. *Nature* **2004**, *427*, 527. (c) Gilbertson, J. D.; Szymczak, N. K.; Tyler, D. R. *J. Am. Chem. Soc.* **2005**, *127*, 10184.
(11) Fryzuk, M. D. *Acc. Chem. Res.* **2009**, *42*, 127.
(12) Knobloch, D. J.; Lobkovsky, E.; Chirik, P. J. *Nat. Chem.* **2010**, *2*, 30.
(13) For an early exampleof an ill-defined titanium complex, see: Sobota, P.; Janas, Z. *J. Organomet. Chem.* **1984**, *276*, 171.
(14) Knobloch, D. J.; Lobkovsky, E.; Chirik, P. J. *J. Am. Chem. Soc.* **2010**, *132*, 10553.
(15) Knobloch, D. J.; Lobkovsky, E.; Chirik, P. J. *J. Am. Chem. Soc.* **2010**, *132*, 15340.
(16) Knobloch, D. J.; Lobkovsky, E.; Chirik, P. J. *J. Am. Chem. Soc.* **2011**, *133*, 10406.
(17) Zhang, X.; Butschke, B.; Schwarz, H. *Chem.—Eur. J.* **2010**, *16*, 12564.
(18) Marsella, J.; Curtis, C. J.; Bercaw, J. E.; Caulton, K. G. *J. Am. Chem. Soc.* **1980**, *102*, 7244.
(19) Roddick, D. M.; Fryzuk, M. D.; Seidler, P. F.; Hillhouse, G. L.; Bercaw, J. E. *Organometallics* **1985**, *4*, 97.
(20) Hanna, T. E.; Keresztes, I.; Lobkovsky, E.; Chirik, P. J. *Inorg. Chem.* **2007**, *46*, 1675.
(21) Green, M. L. H.; McCleverty, J. A.; Pratt, L.; Wilkinson, G. *J. Chem. Soc. A* **1961**, 4854.
(22) Evans, W. J.; Grate, J. W.; Hughes, L. A.; Zhang, H.; Atwood, J. L. *J. Am. Chem. Soc.* **1985**, *107*, 3728.
(23) (a) Arnold, P. L.; Turner, Z. R.; Bellabarba, R. M.; Tooze, R. P. *Chem. Sci.* **2011**, 77. (b) Frey, A. S.; Cloke, F. G. N.; Hitchcock, P. B.; Day, I. J.; Green, J. C.; Aitken, G. *J. Am. Chem. Soc.* **2008**, *130*, 13816. (c) Summerscales, O. T.; Cloke, F. G. N.; Hitchcock, P. B.; Green, J. C.; Hazari, N. *Science* **2006**, *311*, 829. (d) Summerscales, O. T.; Cloke, F. G. N.; Hitchcock, P. B.; Green, J. C.; Hazari, N. *J. Am. Chem. Soc.* **2006**, *128*, 9602.